AIP | The Journal of Chemical Physics

Nuclear spatial delocalization silences electron density oscillations in 2-phenyl-ethyl-amine (PEA) and 2-phenylethyl-N,N-dimethylamine (PENNA) cations

Andrew J. Jenkins, Morgane Vacher, Michael J. Bearpark, and Michael A. Robb

Citation: The Journal of Chemical Physics **144**, 104110 (2016); doi: 10.1063/1.4943273
View online: http://dx.doi.org/10.1063/1.4943273
View Table of Contents: http://scitation.aip.org/content/aip/journal/jcp/144/10?ver=pdfcov
Published by the AIP Publishing

Nuclear spatial delocalization silences electron density oscillations in 2-phenyl-ethyl-amine (PEA) and 2-phenylethyl-N,N-dimethylamine (PENNA) cations

Andrew J. Jenkins, Morgane Vacher, Michael J. Bearpark, and Michael A. Robb
Department of Chemistry, Imperial College London, London SW7 2AZ, United Kingdom

(Received 17 November 2015; accepted 23 February 2016; published online 14 March 2016; publisher error corrected 15 March 2016)

We simulate electron dynamics following ionization in 2-phenyl-ethyl-amine and 2-phenylethyl-N,N-dimethylamine as examples of systems where 3 coupled cationic states are involved. We study two nuclear effects on electron dynamics: (i) coupled electron-nuclear motion and (ii) nuclear spatial delocalization as a result of the zero-point energy in the neutral molecule. Within the Ehrenfest approximation, our calculations show that the coherent electron dynamics in these molecules is not lost as a result of coupled electron-nuclear motion. In contrast, as a result of nuclear spatial delocalization, dephasing of the oscillations occurs on a time scale of only a few fs, long before any significant nuclear motion can occur. The results have been rationalized using a semi-quantitative model based upon the gradients of the potential energy surfaces. © *2016 AIP Publishing LLC.* [http://dx.doi.org/10.1063/1.4943273]

I. INTRODUCTION

Light sources now exist to deliver sub-fs sources for single photon ionization of molecules.[1] One target of attosecond science is the real-time observation and control of electron dynamics upon ionization.[2–6] Recent reports of experiments on phenylalanine suggest the observation of charge oscillation on a few tens of femtoseconds time scale.[4,6] We choose to study 2-phenyl-ethyl-amine (PEA) and 2-phenylethyl-N,N-dimethylamine (PENNA) as models for phenylalanine and other amino acids and because they themselves have been the targets of both experimental[7,8] and theoretical work.[9–12] PEA and PENNA are bifunctional (see Fig. 1), with possible ionization of the nitrogen lone pair (lp) or one of the pairs of quasidegenerate π orbitals of the ring system. Thus we have a 3-level system. Electron dynamics leads to charge migration between the nitrogen and the phenyl ring in these cations. In this article, we investigate the effect of the nuclei on electron dynamics.

Oscillating motion of the electron density is due to interference between states of a coherent electronic wavepacket; the period is inversely proportional to the energy gap.[13,14] A particular case of importance in the present study is that of hole-mixing, where the ionic states are linear combinations of 1h configurations.[13,14] In this case, upon ultrafast ionization, a hole created in one orbital forms a coherent superposition of states involving this 1h configuration but also containing 1h configurations corresponding to ionization of other orbitals. The interference of these states causes the hole to oscillate back-and-forth between orbitals, with charge migration occurring when the orbitals are spatially separated; this mechanism has been demonstrated for valence ionization.[9,10,15,16]

In many theoretical studies, nuclear effects on electron dynamics have been ignored (i.e., pure electron dynamics studies use a single, fixed geometry).[9,10,17–20] In this article, we distinguish two nuclear effects: (i) coupled electron-nuclear motion and (ii) nuclear spatial delocalization as a result of the zero-point energy in the neutral molecule. We have developed the methodology to study the first effect with the Ehrenfest method[21] and have shown that coupled electron-nuclear motion can affect the electron dynamics after a few fs without destroying it.[11,22,23] The second effect, that of nuclear spatial delocalization, has been largely neglected in both theory and interpretation of experimental results so far. Despré *et al.*[24] recently studied the effect of vibrational motion on hole migration by distortions along normal modes with a Boltzmann distribution. To study the effect of nuclear spatial delocalization in the vibrational ground state wavepacket, we have recently[25] simulated electron dynamics for an ensemble of 500 distorted geometries sampled from a Wigner distribution. The Wigner distribution is a quantum distribution function, which means that we mimic the distribution of a quantum vibrational wavepacket. Using this approach in studies on para-xylene and polycyclic norbornadiene (PLN), we showed that the ensemble of geometries leads to a spread of oscillation frequencies, causing a dephasing of oscillations and a loss of overall charge migration on a short time scale, before the effect of nuclear motion is significant. In PEA and PENNA, 3 states are involved rather than 2, hence we expect the propensity for decoherence to be even larger.

The symmetric and asymmetric conformers of PENNA, PENNA-V and PENNA-IV, respectively (Weinkauf *et al.*,[7,26] see figures in the supplementary material[27]), have been previously studied theoretically.[9,10,12] These fixed nuclei studies have demonstrated pure electron dynamics, with fast oscillations with a period as short as 8 fs, and similarly fast in PEA (period ~8 fs).[11] In the present paper, we shall demonstrate that, within the Ehrenfest approximation, coupled electron-nuclear motion *per se* does not destroy the coherent

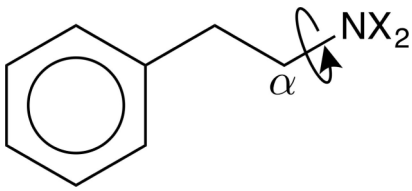

FIG. 1. Structures of PEA (X=H) and PENNA (X=CH_3). Studied conformers differ by rotation around indicated bond. Phenylalanine differs from PEA in the addition of COOH on the α carbon.

oscillations up to ~20 fs in PEA (symmetric conformer V[27]) and both conformers of PENNA, but the natural nuclear spatial delocalization leads to a loss of oscillatory charge migration in a few fs.

We can model charge migration theoretically by solving the electronic time-dependent Schrödinger equation (TDSE). Assuming prompt ionization, the ion is created in a coherent superposition of n states ψ_k at the equilibrium geometry of the neutral. The time-dependent electronic wavefunction can be written (in atomic units),

$$\Psi(\mathbf{r},t;\mathbf{R}) = \sum_{k=1}^{n} c_k e^{-iE_k(\mathbf{R})t}\psi_k(\mathbf{r};\mathbf{R}), \tag{1}$$

where c_k are the initial coefficients of the states. The property of interest, the time-dependent electronic density, reads

$$\rho(r) = \sum_{k=1}^{n} |c_k|^2 \rho_{kk}(r;\mathbf{R}) + \sum_{k=1}^{n-1}\sum_{l>k}^{n} 2\,Re\left(c_k^* c_l \exp(-i\Delta E_{kl}(\mathbf{R})t)\rho_{kl}(r;\mathbf{R})\right), \tag{2}$$

where

$$\rho_{ij}(r;\mathbf{R}) = \int \psi_i^*(\mathbf{r};\mathbf{R})\psi_j(\mathbf{r};\mathbf{R})\, dr^{N-1}. \tag{3}$$

The mixed terms above correspond to the off-diagonal elements of the electronic density matrix; the electronic coherences. Assuming real wavefunctions and real initial coefficients, the oscillatory nature of the coherences can be seen,

$$C(r,t) \approx \sum_{k=1}^{n-1}\sum_{l>k}^{n} 2c_k c_l \cos(\Delta E_{kl}(\mathbf{R})t)\ \ \rho_{kl}(r;\mathbf{R}). \tag{4}$$

Therefore the individual oscillations arising from coherence terms involving each pair of states contribute to the overall electron density "signal" (as shown in Eq. (2)), with periods (T_{kl} in Eq. (5)) inversely proportional to the energy gap between the states in the coherence term

$$T_{kl}(\mathbf{R}) = \frac{2\pi}{\Delta E_{kl}(\mathbf{R})}. \tag{5}$$

II. COMPUTATIONAL DETAILS

A. Electronic structure

In order to study this charge migration computationally, we obtain a set of states from a complete active space self-consistent field (CASSCF) calculation and propagate the TDSE using this basis. In the PEA and PENNA cations, three states are close in energy and involve ionization out of the quasi-degenerate HOMO/HOMO-1 π orbitals of the phenyl ring and the nitrogen lp(2p). These orbitals are therefore included in the CASSCF active space. Correlating orbitals in the form of the corresponding antibonding π orbitals and a nitrogen lp(3p)* orbital are also included. This requires augmenting the standard 6-31G* basis with an additional N centered lp(3p)* function, denoted 6-31G*+3p; the efficacy of this approach has been shown previously.[11,28,29] The resulting CASSCF calculation involves 5 electrons in 6 orbitals, state averaging equally over the three lowest states. Further discussion is provided in S2 of the supplementary material.[27]

B. Initial conditions

Our study assumes that a coherent superposition of states has been populated after ionization, independent of the experimental setup. The initial superposition of adiabatic states is created by choosing a diabatic state corresponding to ionization of a specific orbital. In general, the adiabatic eigenstates are a superposition of such diabatic states and vice versa, so ionization from a diabatic state generates a superposition of adiabatic eigenstates. The diabatic state chosen in the present work corresponds to ionization of the nitrogen 2p lone pair. This is created by localizing[30] the N lone pair orbital. The alternative would be to ionize a ring π orbital (as used in other studies[9,10]). However, the quasi-degenerate π orbitals differ greatly across a distribution of geometries, so such a choice is only unambiguous at a high symmetry. In section 3[27] of the supplementary material, we show that at the neutral minimum geometry of PENNA-V, ionization from the N lone pair (Fig. S1) versus the HOMO π orbital (Fig. S2) leads to electron dynamics (spin density oscillations) that are of the same period and magnitude, just exactly out of phase, supporting our choice.

Upon diabatic ionization of the nitrogen 2p lone pair, the initial populations of the adiabatic states are given by the absolute square of the coefficient of the N-ionized diabatic state within the adiabatic state. For example, in PEA, State 1: 0.97 $|\pi(a')$ ionized$\rangle$ +0.29 |N ionized$\rangle$, State 3: −0.30 $|\pi(a')$ ionized$\rangle$ +0.90 |N ionized$\rangle$ (State 2 is $\pi(a'')$ ionized). Taking the absolute square of the coefficient of the N-ionized diabatic state leads to the populations given in Table I.

The interaction between the cation and the outgoing electron is not included. This sudden removal of an electron, i.e., the sudden ionization approximation, is valid when using

TABLE I. Initial population of each adiabatic eigenstate resulting from diabatic ionization of the nitrogen 2p lone pair at the neutral minimum geometry.

	Initial population		
	State 1	State 2	State 3
PEA	0.09	0.00	0.82
PENNA-IV	0.75	0.01	0.16
PENNA-V	0.48	0.00	0.46

high energy photons such that the electron "quickly" leaves, limiting its interaction with the cation. For this reason, it is currently widely used in the community (for example Refs. 9, 24, and 31).

C. Analysis

While propagating the wavefunction, we follow the charge oscillation by monitoring the spin density, i.e., the difference between the density of α and β spin electrons, as it is a more sensitive indicator than the total electron density. This can subsequently be partitioned on to the atomic sites using Mulliken analysis.[32]

D. Effects of the nuclei

Coupled electron-nuclear motion is studied with our Ehrenfest mixed quantum-classical dynamics implementation;[33] details of which have been described previously.[21] This has now been extended to allow the study of more than 2 states. Nuclear motion is treated classically, using a Hessian-based predictor-corrector algorithm,[34] with a mass-weighted step size of 0.0075 amu$^{\frac{1}{2}}$ bohr (corresponding to a time step of approximately 0.06 fs).

To study spatial nuclear delocalization, electron dynamics is initiated at a range of geometries that span the natural distribution in the ground state nuclear wavepacket. The nuclear wavepacket is represented by sampling a Wigner distribution around the neutral equilibrium geometry. This is a quantum distribution function in classical phase space and creates distortions in all normal modes of the neutral molecule. This distribution is sampled with 500 geometries generated using NewtonX.[35] The results depend on the number of sampled geometries considered, therefore one must make sure that enough distorted geometries are taken into account to sample the distribution and that convergence has been reached.

III. RESULTS AND DISCUSSION

A. Electron dynamics with fixed nuclei

Initiating pure electron dynamics (fixed nuclei) at neutral minimum geometries of PEA and PENNA-V, (diabatic) ionization of the nitrogen 2p lone pair leads to hole mixing between states 1 and 3. These states are a linear combination of the 1h configurations involving ionization of the N lone pair and, due to C_s symmetry, only one (a') of the quasi-degenerate π orbitals of the ring. The initial populations of the states are given in Table I. In the subsequent electron dynamics, charge oscillates between the nitrogen and the ring with a period related to the energy gap between the states (period T_{13} and energy gap ΔE_{13} given in Table II). This oscillatory charge migration in PENNA-V is demonstrated by visualizing the spin density (see Fig. 2 (Multimedia view)), and, for ease of analysis, the same spin density oscillation is shown after partitioning the density on to atomic sites (Fig. 3). The corresponding spin density oscillation in PEA, after partitioning onto atomic sites, is shown in Fig. 4. Note

TABLE II. Properties of the cationic states in PEA and PENNA at the neutral equilibrium geometries, and of a distorted geometry of PENNA-IV. Energy gaps (ΔE), expected periods of oscillations (T) (Eq. (5)) and magnitude of the gradient differences (d) between states of the cation calculated using CASSCF(5,6)/6-31G*+3p. The insensitivity of the energy gaps to correlation effects has been demonstrated with large active space computations.[27] $t_{\frac{1}{2}}$ is the estimated half-life of the average oscillation when using an ensemble of geometries.

			PENNA-IV	
	PEA	PENNA-V	Minimum	Distorted
ΔE_{12} (eV)	0.16	0.51	0.19	0.63
ΔE_{23} (eV)	0.90	0.37	0.04	0.10
ΔE_{13} (eV)	1.07	0.87	0.24	0.73
T_{12} (fs)	25.2	8.2	21.5	6.6
T_{23} (fs)	4.6	11.3	95.5	43.7
T_{13} (fs)	3.9	4.7	17.6	5.7
d_{12}	0.19	0.16	0.29	...
d_{23}	0.15	0.17	0.44	...
d_{13}	0.13	0.09	0.20	...
$t_{\frac{1}{2}}$ (fs)	~1.7	~2.6	~2.5	...

that the superimposed very fast, small amplitude oscillations in the spin density, (and in the case of PEA, a slight modulation of the signal) are due to minor population of more highly excited states that arise from the pure diabatic ionization of the nitrogen lone pair.

Now let us consider PENNA-IV, which has no symmetry. Here, slight hole-mixing occurs between all 3 states (involving the 1h configurations corresponding to ionization of the nitrogen lone pair and both phenyl π orbitals). For this example, we have 3 energy gaps that are important and thus 3 frequencies contribute to the spin density signal with a magnitude proportional to ρ_{kl} (see Eq. (2)).

Using the information in Tables II and III, Eq. (4) can be estimated to show the magnitudes of the multiple oscillations contributing to the overall spin density signal on the nitrogen,

$$C_N(r,t) \approx 0.010\cos(\Delta E_{12}t) + 0.002\cos(\Delta E_{23}t) + 0.214\cos(\Delta E_{13}t). \quad (6)$$

The model predicts a very large amplitude contribution to the spin density signal with period T_{13} = 17.5 fs, with the other

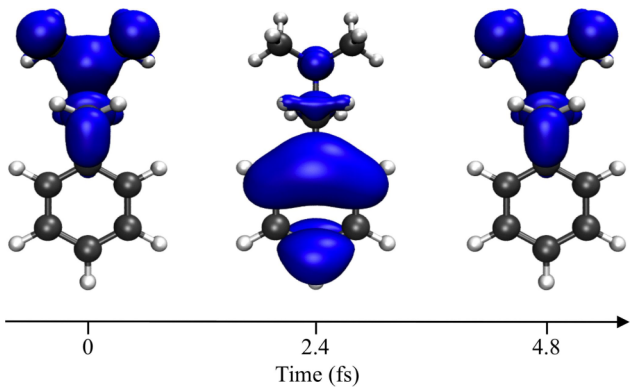

FIG. 2. Spin densities (difference between α and β electron densities) from a fixed nuclei electron dynamics simulation for PENNA-V. Shown are the densities at t = 0, t = T/2 and t = T. (Multimedia view) [URL: http://dx.doi.org/10.1063/1.4943273.1]

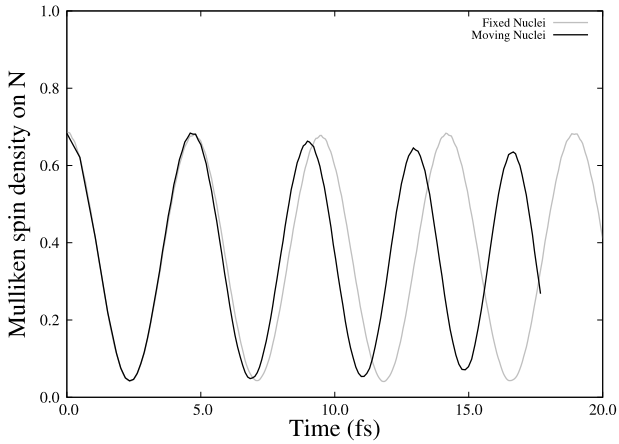

FIG. 3. Simulated Mulliken spin density migration for PENNA-V for the cases of fixed and moving nuclei.

two frequencies only contributing minutely. The simulated spin density for PENNA-IV is shown in Fig. 5 (in the same manner as Figs. 3 and 4). This shows in PENNA-IV the dominant oscillation has a much longer period ~17.5 fs and the maxima are at a slightly different spin density values. This indicates a much slower oscillation also contributing to the signal, in agreement with Table II and Eq. (6).

B. Effect of coupled nuclear motion

As mentioned above, the effect of coupled electron-nuclear motion on the electron dynamics in PEA/PENNA is probed with our Ehrenfest dynamics implementation.[21,33] The resulting spin density on the nitrogen is also plotted in Figs. 3-5, allowing direct comparison to the fixed nuclei case. These figures show that coupled electron-nuclear motion clearly affects the electron dynamics after ~5 fs (in agreement with our previous simulations of methyl substituted benzenes[23]), decreasing the period in the PENNA conformers while increasing both the period and amplitude in PEA. Importantly, in the molecules we have studied, coupled electron-nuclear motion modifies but does not destroy the oscillation in spin density on this time scale.

TABLE III. Adiabatic coefficients c_k and transition density ρ_{kl} at the nitrogen position, estimated by comparing the spin density on the nitrogen for equal superpositions of states k and l with different relative phases.

	PENNA-IV	
	Minimum	Distorted
$\|c_1\|$	0.87	0.18
$\|c_2\|$	0.08	0.69
$\|c_3\|$	0.39	0.61
$\rho_{12}(N)$	~0.15	~0.29
$\rho_{23}(N)$	~0.07	~0.78
$\rho_{13}(N)$	~0.63	~0.72

C. Effect of nuclear spatial delocalization

We now turn to the second important nuclear effect, that of nuclear spatial delocalization as a result of the zero-point energy in the neutral molecule. In the previous work with some 2-level examples,[25] we showed that the Wigner distribution of geometries leads to a corresponding distribution in the energy gaps between cationic states. As a consequence, in the corresponding electron dynamics, the oscillations in electron density occur with varying frequency. Thus the oscillations dephase, leaving no observable overall oscillation in the electron density, with the hole becoming delocalized over the orbitals involved. In the present study, at the distorted geometries of all 3 molecules, hole-mixing occurs between 3 states (PEA and PENNA-V lose their symmetry), meaning all 3 energy gaps contribute to the spin density signal for *each* geometry. A clear example of multiple contributing frequencies is shown in Fig. 6 for a distorted geometry of PENNA-IV (the geometry is defined in section S4[27] of the supplementary material). As at the minimum, the magnitudes of the contributions to the spin density oscillation can be estimated,

$$C_N(r,t) \approx 0.066\cos(\Delta E_{12}t) + 0.215\cos(\Delta E_{23}t) + 0.062\cos(\Delta E_{13}t). \quad (7)$$

This predicts two frequencies contributing with a similar magnitude and frequency ~6 fs, overlaid on a large amplitude

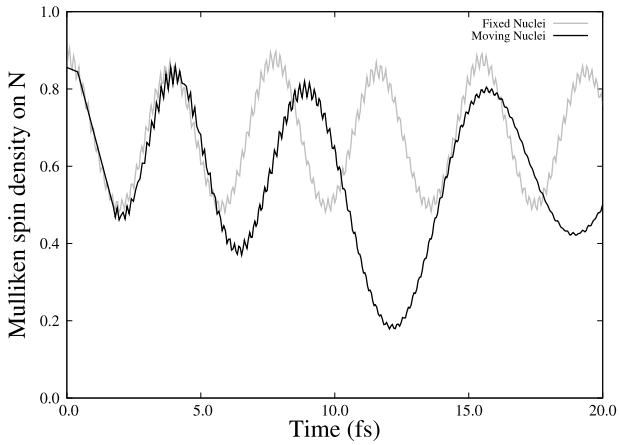

FIG. 4. Simulated Mulliken spin density migration for PEA for the cases of fixed and moving nuclei.

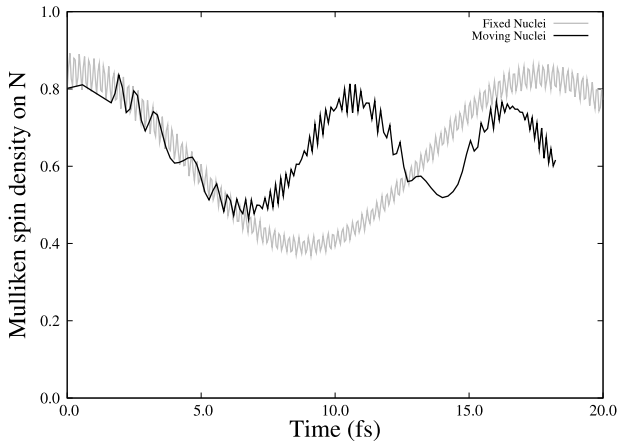

FIG. 5. Simulated Mulliken spin density migration for PENNA-IV for the cases of fixed and moving nuclei.

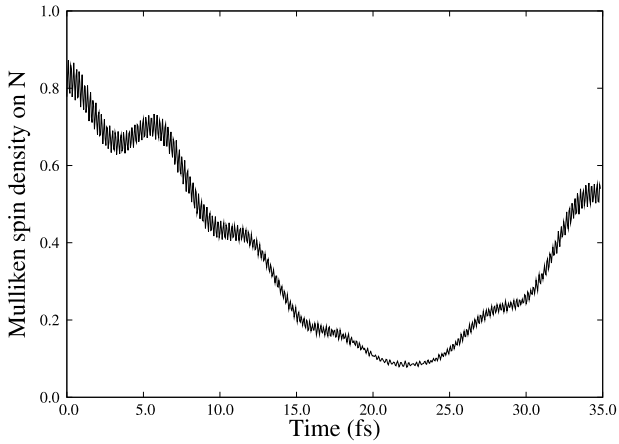

FIG. 6. Fixed nuclei electron dynamics simulation of PENNA-IV cation carried out at one of the geometries in the Wigner distribution around neutral PENNA-IV.

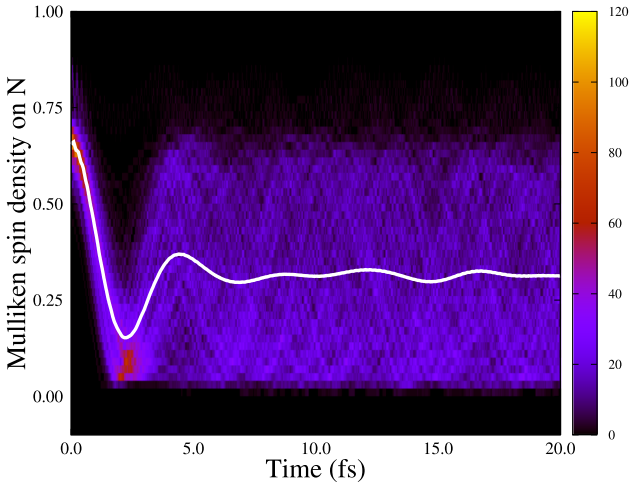

FIG. 8. Sampled electron dynamics for PENNA-V.

contribution with period $T_{13} = 43.7$ fs. These contributions are visible in the simulated electron dynamics at this geometry, see Fig. 6.

The results of electron dynamics (fixed nuclei) simulations, simulated individually at 500 distorted geometries, are shown in Figures 7–9, with the white line indicating the average signal. For PEA and PENNA-V, the average spin density shows only a single damped oscillation before a dephasing occurs, occurring slightly quicker in PEA than PENNA-V. The overall spin density becomes delocalized over the nitrogen and the phenyl ring. In PENNA-IV, dephasing occurs on the same time scale as PENNA-V but, due to its longer period, the average spin density shows only a fraction of an oscillation before the signal is averaged out: the overall spin density becomes delocalized. These show the spatial delocalization of the nuclei leads to dephasing of the oscillations in a few fs (an estimate of the half-life of the spin density oscillation, $t_{\frac{1}{2}}$ (Table II), can be made by fitting a gaussian decay to the average spin density).

D. Rationalization using gradient differences

The presence of more than one contributing frequency complicates the analytical model of dephasing detailed in our previous study.[25] Therefore, for the 3-state case, there is no simple analytical model but it is helpful to consider the main physical factors affecting the dephasing. For a gaussian distribution in the nuclear coordinates around the neutral equilibrium geometry, the energy gaps between the 3 cationic states will vary. An indication of how quickly the energy gaps will change is given by the magnitude of the gradient differences of the states $d_{kl} = |\frac{\partial(E_k - E_l)}{\partial \mathbf{R}}|$. Therefore, intuitively, the greater the magnitude of the gradient difference, the wider the distribution of energy gaps. This gives a wider distribution of oscillation frequencies and a quicker dephasing time. Equally, the wider the gaussian distribution of geometries, the quicker the dephasing. In summary, the dephasing effect is general but the time scale is system dependent, and may be slow in certain cases.[24,25]

For the 3 molecules studied here, the magnitude of the gradient differences calculated at the (neutral) equilibrium geometry are given in Table II. The magnitude of the gradient difference of the dominant oscillation in PEA (involving states 1 and 3, d_{13}), is greater than that in PENNA-V (d_{13}), therefore suggesting PEA should have a quicker dephasing time. PEA and PENNA-V have a very similar conformation but the nature of their electron dynamics is dramatically affected by

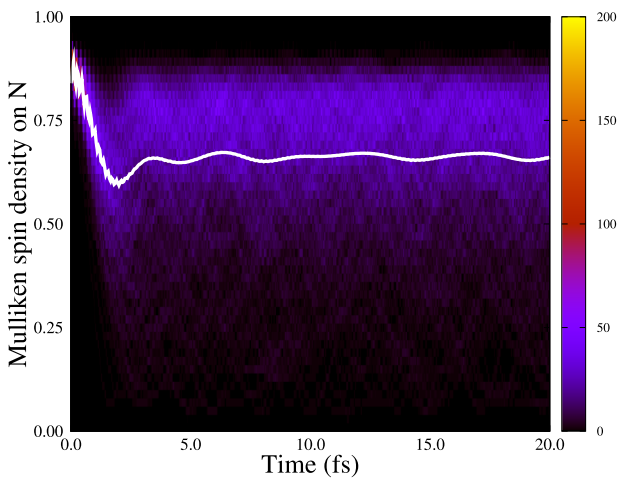

FIG. 7. Sampled electron dynamics for PEA.

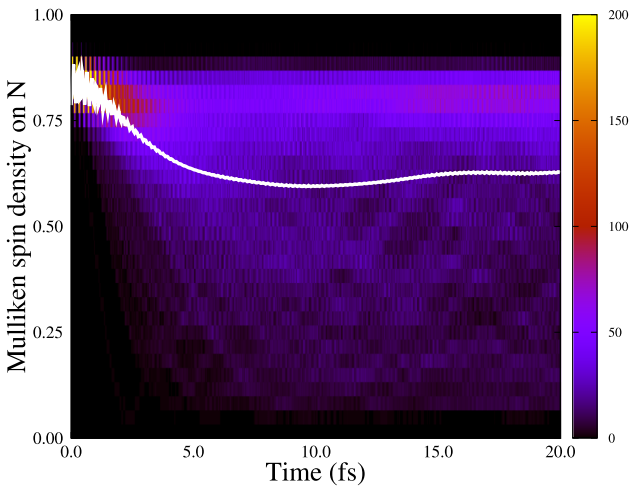

FIG. 9. Sampled electron dynamics for PENNA-IV.

the position of atoms around the nitrogen. In PEA, these are hydrogens, whose position varies more than the heavy carbons in PENNA when considering a Wigner distribution. This gives a wider distribution of geometries in PEA, a greater spread of oscillation frequencies, and results in quicker dephasing in PEA than in PENNA-V, as seen in Figures 7 and 8 and the estimated dephasing time in Table II. PENNA-IV has larger gradient differences than PENNA-V, however, PENNA-IV has cationic states that are less strongly mixed. This means its spin density signal for each geometry (although it still has contributions from several pairs of states) is dominated by a smaller number of states than in PENNA-V. This effect partly negates that of the gradient differences, resulting in the conformers showing approximately the same dephasing time.

IV. CONCLUSION

In the present work, we have studied the effect of both coupled electron-nuclear motion and nuclear delocalization on electron dynamics in PEA and two conformers of PENNA. Within the Ehrenfest approximation, our calculations show that oscillatory electron dynamics in these molecules is not lost as a result of coupled electron-nuclear motion, rather, it is lost as a result of nuclear delocalization due to the zero-point energy in the neutral molecule. The delocalization leads to dephasing of the oscillations to occur on a very short time scale, far before any significant nuclear motion. This dephasing occurs on a similar time scale for PEA and the two lowest energy conformers of PENNA. The dephasing occurs on a shorter time scale than in para-xylene and PLN[25] due to the specific form of the cationic states (larger gradient differences) but also because more than 2 states are close in energy and are involved in the electron dynamics.

These results and those in our previous study[25] suggest one could not observe long-lived electron dynamics in PEA, PENNA and similar systems. The physical model involving the computed gradient differences between the coupled states seems to be a useful predictor.

ACKNOWLEDGMENTS

This work was supported by UK-EPSRC Grant No. EP/I032517/1. All calculations were run using the Imperial College High Performance Computing service.

[1]D. Fabris, T. Witting, W. A. Okell, D. J. Walke, P. Matia-Hernando, J. Henkel, T. R. Barillot, M. Lein, J. P. Marangos, and J. W. G. Tisch, Nat. Photonics **9**, 383 (2015).
[2]M. F. Kling and M. J. Vrakking, Annu. Rev. Phys. Chem. **59**, 463 (2008).
[3]F. Krausz and M. Ivanov, Rev. Mod. Phys. **81**, 163 (2009).
[4]L. Belshaw, F. Calegari, M. J. Duffy, A. Trabattoni, L. Poletto, M. Nisoli, and J. B. Greenwood, J. Phys. Chem. Lett. **3**, 3751 (2012).
[5]F. Lépine, M. Y. Ivanov, and M. J. J. Vrakking, Nat. Photonics **8**, 195 (2014).
[6]F. Calegari, D. Ayuso, A. Trabattoni, L. Belshaw, S. De Camillis, S. Anumula, F. Frassetto, L. Poletto, A. Palacios, P. Decleva, J. B. Greenwood, F. Martin, and M. Nisoli, Science **346**, 336 (2014).
[7]R. Weinkauf, L. Lehr, and A. Metsala, J. Phys. Chem. A **107**, 2787 (2003).
[8]L. Lehr, T. Horneff, R. Weinkauf, and E. W. Schlag, J. Phys. Chem. A **109**, 8074 (2005).
[9]S. Lünnemann, A. I. Kuleff, and L. S. Cederbaum, J. Chem. Phys. **129**, 104305 (2008).
[10]S. Lünnemann, A. I. Kuleff, and L. S. Cederbaum, Chem. Phys. Lett. **450**, 232 (2008).
[11]D. Mendive-Tapia, M. Vacher, M. J. Bearpark, and M. A. Robb, J. Chem. Phys. **139**, 044110 (2013).
[12]B. Mignolet, R. D. Levine, and F. Remacle, J. Phys. B: At., Mol. Opt. Phys. **47**, 124011 (2014).
[13]J. Breidbach and L. S. Cederbaum, J. Chem. Phys. **118**, 3983 (2003).
[14]A. I. Kuleff and L. S. Cederbaum, J. Phys. B: At., Mol. Opt. Phys. **47**, 124002 (2014).
[15]A. I. Kuleff, J. Breidbach, and L. S. Cederbaum, J. Chem. Phys. **123**, 044111 (2005).
[16]H. Hennig, L. S. Cederbaum, and J. Breidbach, J. Phys. Chem. A **109**, 8 (2005).
[17]F. Remacle and R. D. Levine, Z. Phys. Chem. **221**, 647 (2007).
[18]A. I. Kuleff and L. S. Cederbaum, Chem. Phys. **338**, 320 (2007).
[19]G. Periyasamy, R. D. Levine, and F. Remacle, Chem. Phys. **366**, 129 (2009).
[20]A. I. Kuleff, S. Lünnemann, and L. S. Cederbaum, J. Phys. Chem. A **114**, 8676 (2010).
[21]M. Vacher, D. Mendive-Tapia, M. J. Bearpark, and M. A. Robb, Theor. Chem. Acc. **133**, 1 (2014).
[22]M. Vacher, M. J. Bearpark, and M. A. Robb, J. Chem. Phys. **140**, 201102 (2014).
[23]M. Vacher, D. Mendive-Tapia, M. J. Bearpark, and M. A. Robb, J. Chem. Phys. **142**, 094105 (2015).
[24]V. Despré, A. Marciniak, V. Loriot, M. C. E. Galbraith, A. Rouzée, M. J. J. Vrakking, F. Lépine, and A. I. Kuleff, J. Phys. Chem. Lett. **6**, 426 (2015).
[25]M. Vacher, L. Steinberg, A. J. Jenkins, M. J. Bearpark, and M. A. Robb, Phys. Rev. A **92**, 040502 (2015).
[26]R. Weinkauf, F. Lehrer, E. W. Schlag, and A. Metsala, Faraday Discuss. **115**, 363 (2000).
[27]See supplementary material at http://dx.doi.org/10.1063/1.4943273 for structural information, alternate initial conditions, and large active space study.
[28]M. Boggio-Pasqua, M. J. Bearpark, M. Klene, and M. A. Robb, J. Chem. Phys. **120**, 7849 (2004).
[29]V. Santolini, J. P. Malhado, M. A. Robb, M. Garavelli, and M. J. Bearpark, Mol. Phys. **113**, 1978 (2015).
[30]S. F. Boys, in *Quantum Theory of Atoms, Molecules, and the Solid State*, edited by P.-O. Lowdin (Academic, New York, 1966), pp. 253–262.
[31]A. I. Kuleff, S. Lünnemann, and L. S. Cederbaum, Chem. Phys. **414**, 100 (2013).
[32]R. S. Mulliken, J. Chem. Phys. **23**, 1833 (1955).
[33]M. J. Frisch, G. W. Trucks, H. B. Schlegel, G. E. Scuseria, M. A. Robb, J. R. Cheeseman, G. Scalmani, V. Barone, B. Mennucci, G. A. Petersson, H. Nakatsuji, M. Caricato, X. Li, H. P. Hratchian, A. F. Izmaylov, J. Bloino, G. Zheng, J. L. Sonnenberg, W. Liang, M. Hada, M. Ehara, K. Toyota, R. Fukuda, J. Hasegawa, M. Ishida, T. Nakajima, Y. Honda, O. Kitao, H. Nakai, T. Vreven, J. A. Montgomery, Jr., J. E. Peralta, F. Ogliaro, M. Bearpark, J. J. Heyd, E. Brothers, K. N. Kudin, V. N. Staroverov, T. Keith, R. Kobayashi, J. Normand, K. Raghavachari, A. Rendell, J. C. Burant, S. S. Iyengar, J. Tomasi, M. Cossi, N. Rega, J. M. Millam, M. Klene, J. E. Knox, J. B. Cross, V. Bakken, C. Adamo, J. Jaramillo, R. Gomperts, R. E. Stratmann, O. Yazyev, A. J. Austin, R. Cammi, C. Pomelli, J. W. Ochterski, R. L. Martin, K. Morokuma, V. G. Zakrzewski, G. A. Voth, P. Salvador, J. J. Dannenberg, S. Dapprich, P. V. Parandekar, N. J. Mayhall, A. D. Daniels, O. Farkas, J. B. Foresman, J. V. Ortiz, J. Cioslowski, and D. J. Fox, Gaussian Development Version, Revision H.32, 2010.
[34]J. M. Millam, V. Bakken, W. Chen, W. L. Hase, and H. B. Schlegel, J. Chem. Phys. **111**, 3800 (1999).
[35]M. Barbatti, G. Granucci, H. Lischka, M. Persico, and M. Ruckenbauer, Newton-X: A Package for Newtonian Dynamics Close to the Crossing Seam, Version 0.11b, 2006, www.univie.ac.at/newtonx.